Supporting Information for

ORIGINAL ARTICLE

DT-13 ameliorates LPS-induced acute lung injury via targeting NMMHC IIA to modulate FOXO1/ KLF2/ SPHK1 pathway

Jiazhi Zhang[1,#], Jiahui Tang[1,#], Huifen Ma[1], Ziqian Pan[1], Mengxue Xiao[1], Jianhao Zhou[1], Ling Zhang[1] , Shuaishuai Gong[1], Fang Li[1], Boyang Yu[1,*], Yuanyuan Zhang[1,*], Junping Kou[1,*]

[1]State Key Laboratory of Natural Medicines, Jiangsu Key Laboratory of TCM Evaluation and Translational Research, Department of Pharmacology of Chinese Materia Medica, School of Traditional Chinese Pharmacy, China Pharmaceutical University, Nanjing 211198, China

Running title: DT-13 ameliorates ALI via targeting NMMHC IIA

# Jiazhi Zhang and Jiahui Tang contributed equally to this work.

Correspondence

Junping Kou, Yuanyuan Zhang, and Boyang Yu,

State Key Laboratory of Natural Medicines,

Jiangsu Key Laboratory of TCM Evaluation and Translational Research,

Department of Pharmacology of Chinese Materia Medica,

School of Traditional Chinese Pharmacy,

China Pharmaceutical University, Nanjing 211198, China.

E-mail: junpingkou@cpu.edu.cn (Junping Kou);

yuanyuanzhang@cpu.edu.cn (Yuanyuan Zhang);

boyangyu 59@163.com (Boyang Yu);

METHODS

Untargeted Metabolomics Analysis

Sample Pretreatment

The serum of mice was collected 6 h after LPS exposure. After standing for about 60 min, the blood was centrifuged with 3,500 $r \cdot min^{-1}$ for 10 min at 15°C. The obtained serum samples were sub-packed and stored at -80°C until the analysis. 200 μL of serum were used for untargeted metabolomics analysis and 600 μL of methanol was added into samples for precipitating protein. Samples were subsequently centrifuged (13,000 rpm, 15 min) at 4°C followed by swirling 60 s. The supernatant was transferred to a tube and dried under a gentle stream of nitrogen at room temperature. Then, the residue was dissolved with 200 μl methanol and centrifuged (13,000 rpm, 15 min) at 4°C for further analysis.

HPLC-Q-TOF/MS Analysis

The detection of metabolites in serum samples was performed on an Agilent Technologies 6540 Accurate-Mass Q-TOF LC/MS (United States) with electrospray ionization (ESI) source and the data was collected by a mass hunter workstation. The eluants A and B were deionized water (0.1%, formic acid) and acetonitrile (0.1% formic acid), respectively. Serum analyses were achieved on a SynergiTM Fusion-RP C18 column (50 × 2 mm i.d., 2.5 μm) with a gradient elution program: 0-5 min, 5-5% B; 5-10 min, 5-30% B; 10-15 min, 30-60% B;15-20 min, 60-70 % B; 20-22 min, 70-80% B; 22-25 min, 80-95% B; 25-30 min, 95-95% B. The flow rates were set at 0.2 $ml \cdot min^{-1}$ with an injection volume of 10 μl. The Q-TOF/MS operating parameters were set as follows: fragment voltage, 120 V; nebulizer gas, 35 psig; capillary

voltage, 4,000 V; drying gas flow rate, 9 $L \cdot min^{-1}$; temperature, 325 °C; detection range, m/z 50-1,500 in full scan mass spectra. The MS data acquisition was carried out in positive and negative ionization modes.

Data Analysis of Metabolomics Strategies

Before multivariate analysis, the data format (. mzdata) files obtained by MassHunter Workstation Software (version B.06.00, Agilent Technologies) were processed by XCMS software performing on the R+ package (R Foundation for Statistical Computing, Vienna, Austria), and the data pretreatment procedures include non-linear retention time alignment, peak discrimination, filtering, alignment, and matching. All detected peaks were tabulated with tR-m/z pairs and outputted for statistical analyses. To screen the significant compounds that were responsible for the difference among wild-sham (WS), wild-model (WM), knockdown-sham (TS), and knockdown-model (TM) groups, metabolomic strategies were subsequently used to dispose the data. Principal component analysis (PCA), orthogonal partial least square discriminant analysis (OPLS-DA), volcano Plot, and heatmap developed by Metaboanalyst (https://www.metaboanalyst.ca/) were adopted to do the preliminary screening. PCA is a multivariate technique that can select the typical variables from a data table by several linear transformations, and OPLS-DA is a supervised machine learning model. The online database including HMDB (http://www.hmdb.ca/), METLIN (http://metlin.scripps.edu/), and MassBank (http://www.massbank.jp/) was performed to identify the potential metabolites by matching with the message of ion fragments.

Targeted Analysis for S1P by HPLC-QQQ-MS/MS

Targeted analysis was performed on a triple quadrupole tandem high-performance liquid chromatography-mass spectrometry (HPLC-QQQ-MS/MS) system (Agilent, 6465) with Ketoprofen as the internal standard. Chromatographic separation was performed on a C18 chromatographic column (Agilent Eclipse Plus C18, 2.1 mm × 50 mm, 5 μm) with a gradient elution program: 0-2 min, 25% B; 2-5 min, 25% B; 5-8 min, 40% B; 8-10 min, 40% B; 10-20 min, 50% B. The mobile phase system consists of deionized water containing 0.1% formic acid (A) and acetonitrile containing 0.1% formic acid (B) at a flow rate of 0.3 $ml \cdot min^{-1}$. Multiple reaction monitoring transitions in the positive mode were performed at m/z 380.3→264.3 for the target analyte S1P and m/z 255.1→209 for the internal standard compound. MS parameters for the LC-MS/MS system, including the fragment and voltage collision energy of S1P and internal standard were 110, 21, and 90 V, 17 V, respectively.

Proximity ligation assays (PLA)

A PLA kit (DUO92002, DUO92004, and DUO92008; Sigma–Aldrich) was employed to detect interactions between NMMHC IIA and TLR4 in HUVECs according to the manufacturer's protocols18. Samples were incubated with primary antibodies for NMMHC IIA and TLR4. Secondary antibodies conjugated with oligonucleotides (PLA probes) were added to the reaction for subsequent ligation and rolling circle amplification. Images were observed under a CLSM (LSM700; Zeiss) and processed using ZEN imaging software. PLA were each performed in at least six independent experiments. For each experiment, data were collected from three independently cultured cell wells.

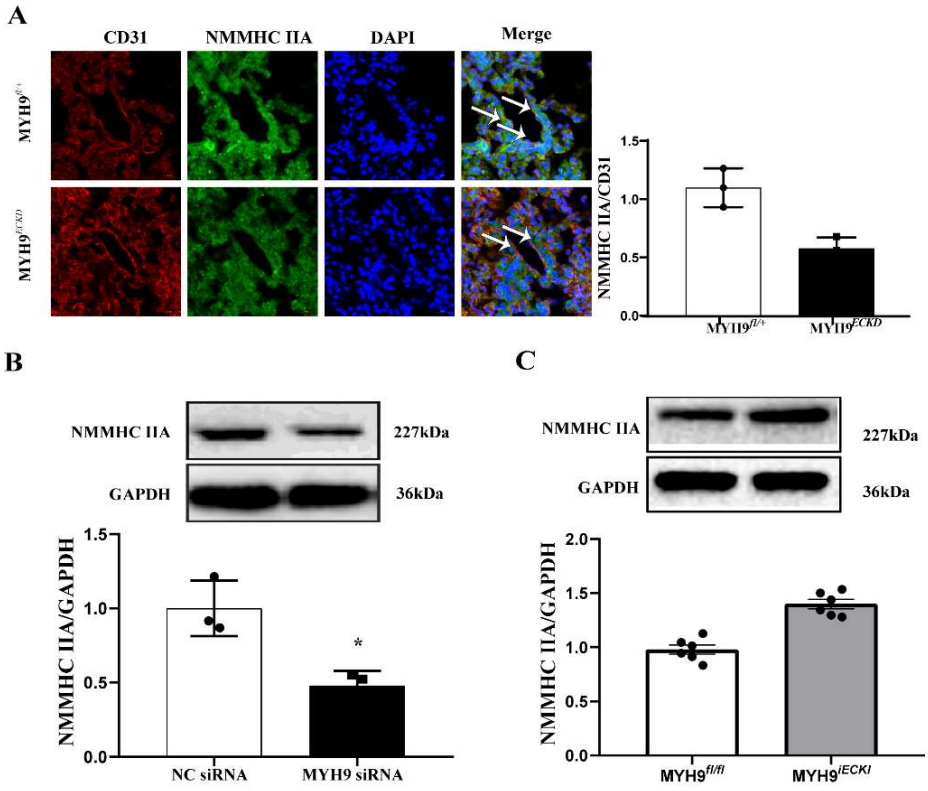

Fig. S1. Identification of knockout and overexpression efficiency of NMMHC IIA in endothelial cells. A. Endothelial-specific monoallelic deletion of NMMHC IIA was analyzed by immunofluorescent co-staining of NMMHC IIA (green) and the endothelial cell marker CD31 (red), nuclei were stained with DAPI (blue). Arrows indicate the colocalization of NMMHC IIA and CD31 (n=3). Scale bar=20 mm. **B.** Western blot analysis of NMMHC IIA expression levels in HUVECs treated with MYH9 siRNA (n=3). **C.** Western blot analysis of NMMHC IIA expression levels in MYH9^{iECKI} mouse lung tissues (n=6).

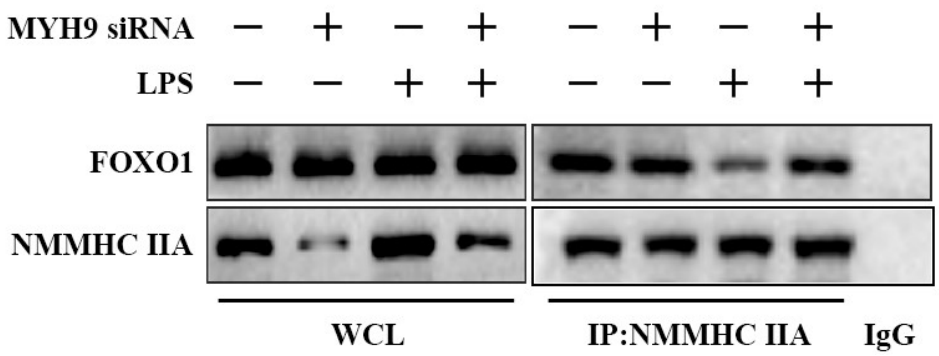

Fig. S2. The LPS-induced dissociation of FOXO1 from NMMHC IIA in HUVECs was diminished by MYH9 siRNA. The interaction of NMMHC IIA and FOXO1 was verified by Co-Immunoprecipitation (Co-IP).

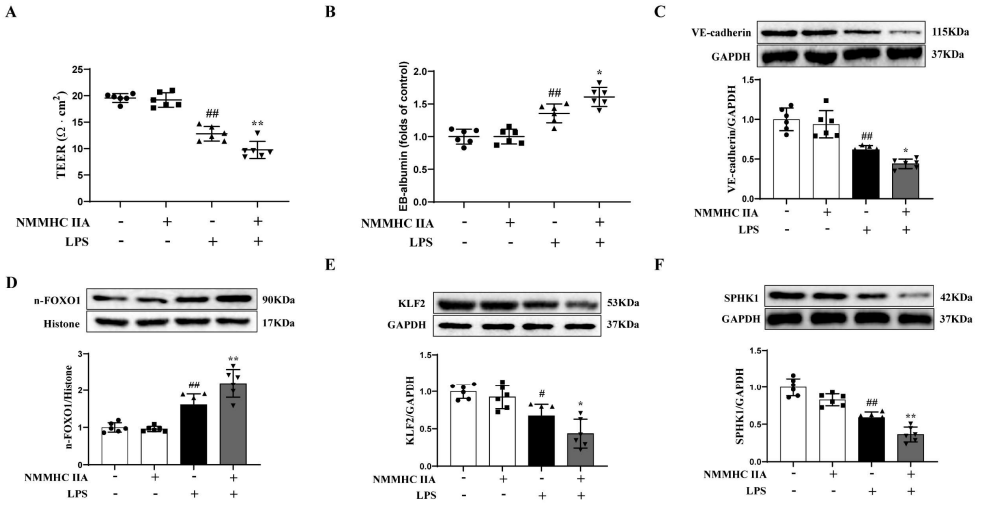

Fig. S3 NMMHC IIA overexpression aggregated LPS-induced impairment of barrier function in HUVECs through modulating FOXO1/KLF2/SPHK1 pathway. A-B. TEER and EBA leakage assays were used to determine the effect of NMMHC IIA overexpression on LPS-induced hyperpermeability(n=6). **C-F.** The expression of VE-cadherin, n-FOXO1, KLF2 and SPHK1 in HUVECs was measured by western blot (n=6). Data are shown as the means ± SD. $^{\#\#}P<0.01$ compared with the control group; $^{*}P<0.05$, $^{**}P<0.01$ compared with the model group.

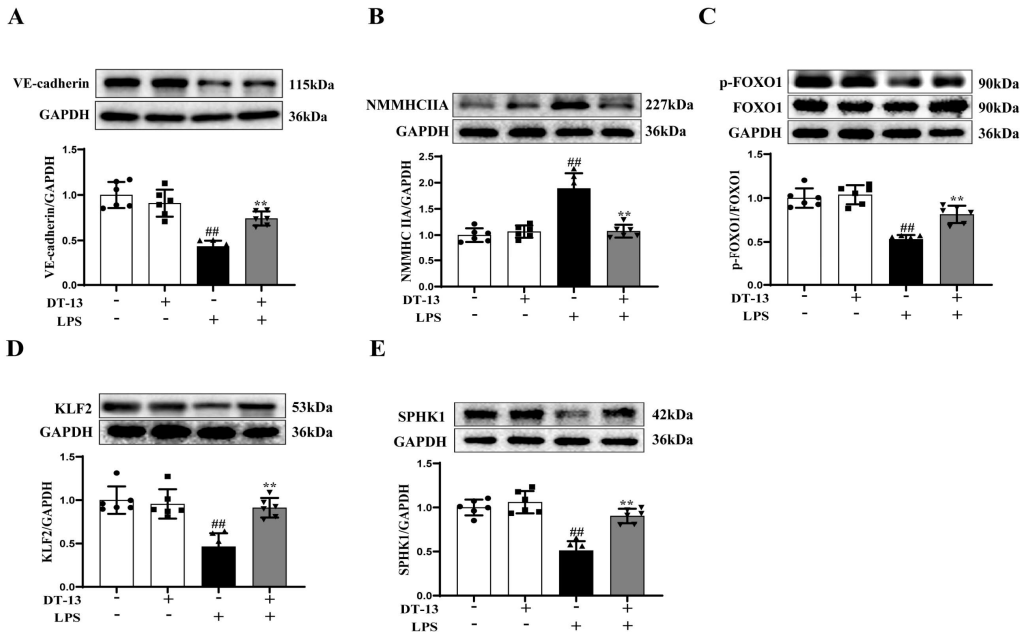

Fig. S4. DT-13 ameliorated LPS-induced lung vascular hyperpermeability in mice through modulating NMMHC IIA/FOXO1/KLF2/SPHK1 pathway. A-E. The expression of VE-cadherin, NMMHC IIA, KLF2, and SPHK1 and the ratio of p-FOXO1/FOXO1 in lung tissues was measured by western blot (n=6). Data are shown as the means ± SD. $^{\#\#}P< 0.01$ compared with the sham group; $^{**}P < 0.01$ compared with the model group.

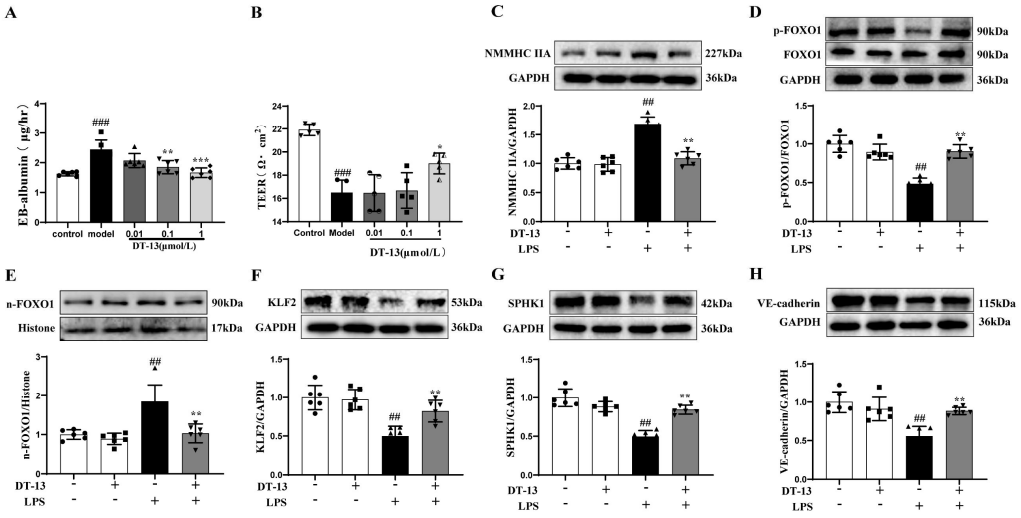

Fig. S5. DT-13 ameliorated LPS-induced impairment of barrier function in HUVECs. **A, B.** EBA leakage assays and TEER were used to determine the effect of DT-13 on LPS-induced hyperpermeability(n=6). **C-H.** The expression of VE-cadherin, NMMHC IIA, n-FOXO1, KLF2, SPHK1, and the ratio of p-FOXO1/FOXO1 in HUVECs was measured by western blot (n=6). Data are shown as the means ± SD. $^{\#\#}P<0.01$ compared with the control group; $^{*}P<0.05$, $^{**}P<0.01$ compared with the model group.

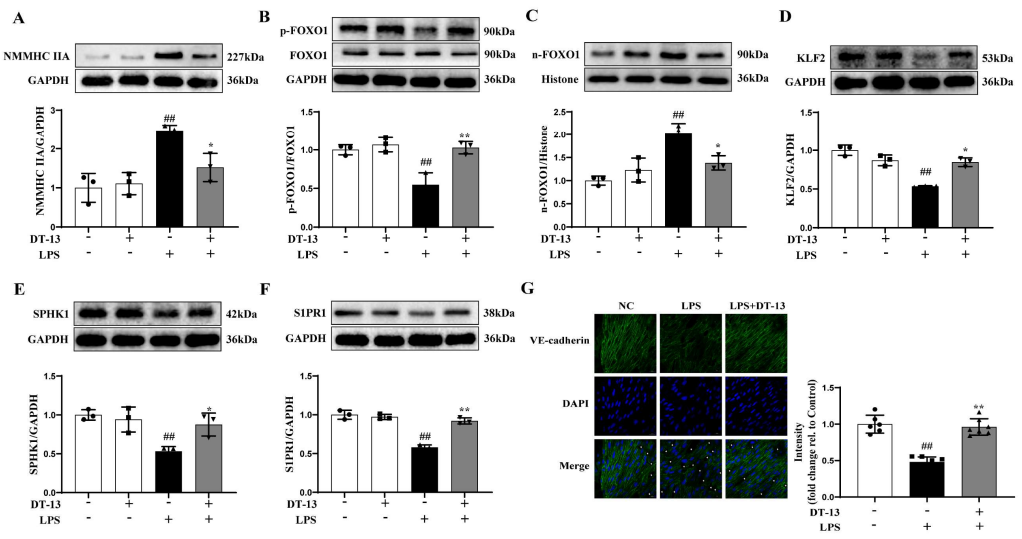

Fig. S6. DT-13 ameliorated LPS-induced impairment of barrier function in murine lung endothelial cells (MLECs) through modulating NMMHC IIA/FOXO1/KLF2/SPHK1 pathway. A-F. The ratio of p-FOXO1/FOXO1 and the expression of NMMHC IIA, n-FOXO1, KLF2, SPHK1, and S1PR1 in MLECs was measured by western blot (n=3). **G.** Immunofluorescence staining for VE-cadherin(green) and nuclei (blue) was performed on MLECs. Scale bar: 5 μm. Data are shown as the means ± SD. $^{\#\#}P<0.01$ compared with the control group; $^{*}P<0.05$, $^{**}P<0.01$ compared with the model group.

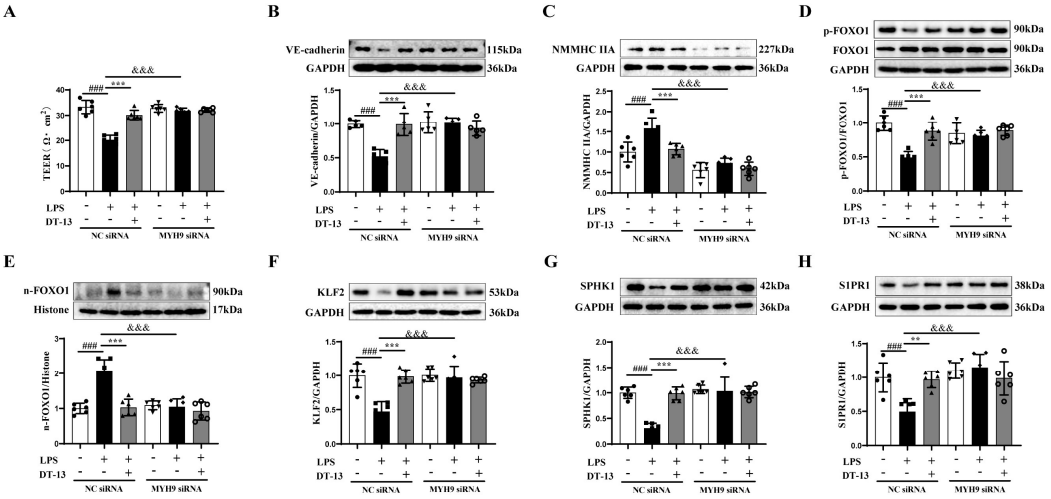

Fig. S7. NMMHC IIA knockdown eliminated the protective effect of DT-13 against LPS-induced impairment of barrier function in HUVECs. A. Transendothelial electrical resistance (TEER) of HUVECs was performed (n=6). **B.** The expression of VE-cadherin in HUVECs was measured by western blot (n=5). **C-H.** The expression of S1PR1, NMMHC IIA, n-FOXO1, KLF2, SPHK1 and the ratio of p-FOXO1/FOXO1 in HUVECs was measured by western blot (n=6).Data are shown as the means ± SD. $^{\#\#\#}P$<0.001 compared with the control group; $^{**}P$<0.01, $^{***}P$<0.001 compared with the model group, $^{\&\&\&}P$ < 0.001 compared with the WT model group.

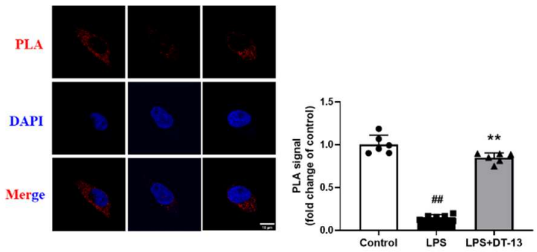

Fig. S8. DT-13 inhibited the LPS-induced dissociation of NMMHC IIA from TLR4 in HUVECs. NMMHC IIA is dissociated from TLR4 after LPS treatment. Confocal microscopy of HUVECs challenged with LPS for 30 min, followed by PLA reaction for NMMHC IIA–TLR4 interactions (red signal) and DAPI (blue) staining. Scale bars = 10 μm. PLA signals were quantified using Image J. Data are expressed as mean ± SD, $n = 6$. $^{\#\#}P < 0.01$ compared with the control group, $^{**}P < 0.01$ compared with the model group.